Propagation of generalized vector Helmholtz-Gauss beams through paraxial optical systems

Raul I. Hernandez-Aranda, Julio C. Gutiérrez-Vega

Photonics and Mathematical Optics Group, Tecnológico de Monterrey, Monterrey, México 64849

juliocesar@itesm.mx

Manuel Guizar-Sicairos

The Institute of Optics, University of Rochester, Rochester, New York 14627

Miguel A. Bandres

California Institute of Technology, Pasadena, California 91125

Abstract: We introduce the generalized vector Helmholtz-Gauss (gVHzG) beams that constitute a general family of localized beam solutions of the Maxwell equations in the paraxial domain. The propagation of the electromagnetic components through axisymmetric ABCD optical systems is expressed elegantly in a coordinate-free and closed-form expression that is fully characterized by the transformation of two independent complex beam parameters. The transverse mathematical structure of the gVHzG beams is form-invariant under paraxial transformations. Any paraxial beam with the same waist size and transverse spatial frequency can be expressed as a superposition of gVHzG beams with the appropriate weight factors. This formalism can be straightforwardly applied to propagate vector Bessel-Gauss, Mathieu-Gauss, and Parabolic-Gauss beams, among others.

OCIS codes: (050.1970) Diffractive optics; (260.5430) Polarization; (350.5500) Propagation; (140.3300) Laser beam shaping.

References and links

1. M. Lax, W. H. Louisell, and W. B. McKnight, "From Maxwell to paraxial wave optics," Phys, Rev. A **11**, 1365–1370 (1975).
2. L. W. Davis and G. Patsakos, "TM and TE electromagnetic beams in free space," Opt. Lett. **6**, 22–23 (1981).
3. Z. Bouchal and M. Olivík, "Non-diffractive vector Bessel beams," J. Mod. Opt. **42**, 1555–1566 (1995).
4. D. G. Hall, "Vector-beam solutions of Maxwell's wave equation," Opt. Lett. **21**, 9–11 (1996).
5. A. A. Tovar and G. H. Clark, "Concentric-circle-grating, surface-emitting laser beam propagation in complex optical systems," J. Opt. Soc. Am. A **14**, 3333–3340 (1997).
6. A. Flores-Pérez, J. Hernández-Hernández, R. Jáuregui, and K. Volke-Sepúlveda, "Experimental generation and analysis of first-order TE and TM Bessel modes in free space," Opt. Lett. **31**, 1732–1734 (2006).
7. K. Volke-Sepulveda and E. Ley-Koo, "General construction and connections of vector propagation invariant optical fields: TE and TM modes and polarization states," J. Opt. A: Pure Appl. Opt., **8**, 867–877 (2006).
8. M. A. Bandres and J. C. Gutiérrez-Vega, "Vector Helmholtz-Gauss and vector Laplace-Gauss beams," Opt. Lett. **30**, 2155–2157 (2005).
9. L. J. Chu, "Electromagnetic waves in elliptic hollow pipes of metal," J. Appl. Phys. **9**, 583–591 (1938).
10. R. D. Spence and C. P. Wells, "The propagation of electromagnetic waves in parabolic pipes," Phys. Rev. **62**, 58–62 (1942).

#73591 - $15.00 USD Received 2 August 2006; revised 15 September 2006; accepted 15 September 2006

11. J. C. Gutiérrez-Vega and M. A. Bandres, "Helmholtz–Gauss waves," J. Opt. Soc. Am. A **22**, 289–298 (2005).
12. C. López-Mariscal, M. A. Bandres, and J. C. Gutiérrez-Vega, "Observation of the experimental propagation properties of Helmholtz-Gauss beams," Opt. Eng. **45**, 068001 (2006).
13. Q. Zhan, "Trapping metallic Rayleigh particles with radial polarization," Opt. Express **12**, 3377-3382 (2004).
14. V. G. Niziev and A. V. Nesterov, "Influence of beam polarization on laser cutting efficiency," J. Phys. D: Appl. Phys. **32**, 1455–1461 (1999).
15. R. Dorn, S. Quabis, and G. Leuchs, "Sharper focus for a radially polarized light beam," Phys. Rev. Lett. **91**, 233901 (2003).
16. Z. Bouchal, "Nondiffracting optical beams: physical properties, experiments, and applications" Czech. J. Phys. **53,** 537-578 (2003).
17. L. W. Casperson, D. G. Hall, and A. A. Tovar, "Sinusoidal–Gaussian beams in complex optical systems," J. Opt. Soc. Am. A **14**, 3341–3348 (1997).
18. S. Ruschin, "Modified Bessel nondiffracting beams," J. Opt. Soc. Am. A **11**, 3224–3228 (1994).
19. M. Santarsiero, "Propagation of generalized Bessel-Gauss beams through ABCD optical systems," Opt. Commun. **132**, 1–7 (1996).
20. S. A. Collins, "Lens-system diffraction integral written in terms of matrix optics," J. Opt. Soc. Am. **60**, 1168–1177 (1970).
21. A. E. Siegman, *Lasers* (University Science, 1986).
22. J. C. Gutiérrez-Vega, M. D. Iturbe-Castillo, and S. Chávez-Cerda, "Alternative formulation for invariant optical fields: Mathieu beams," Opt. Lett. **25**, 1493–1495 (2000).
23. M. A. Bandres, J. C. Gutiérrez-Vega, and S. Chávez-Cerda, "Parabolic nondiffracting optical wave fields," Opt. Lett. **29**, 44–46 (2004).
24. J. A. Stratton, *Electromagnetic theory* (McGraw-Hill, New York, 1941)
25. P. Morse and H. Feshbach, *Methods of Theoretical Physics* (McGraw-Hill, New York, 1953).
26. M. Guizar-Sicairos and J. C. Gutiérrez-Vega, "Generalized Helmholtz-Gauss beams and its transformation by paraxial optical systems," Opt. Lett. **31**, 2912–2914 (2006).

1. Introduction

The problem of finding vector beam solutions of Maxwell equations has been studied by several researchers [1, 2, 3, 4, 5, 6, 7, 8]. In this direction, the existence of the vector Helmholtz-Gauss (vHzG) beams, which constitute a general family of localized electromagnetic beams, was demonstrated theoretically in a recent paper [8] for propagation in free space. Special cases of the vHzG beams are the transverse electric (TE) and transverse magnetic (TM) Gaussian vector beams [2], nondiffracting vector Bessel beams [3], polarized Bessel–Gauss [4], Mathieu-Gauss, and Parabolic-Gauss beams, modes in cylindrical waveguides and cavities [9, 10], and scalar Helmholtz-Gauss beams [11, 12].

In this paper, we introduce a useful generalized form of the vHzG beams that we will refer to as *generalized* vHzG (gVHzG) beams. The paraxial propagation of the gVHzG beams is studied, not only in free space, but also through more general types of paraxial optical systems characterized by complex ABCD matrices, including lenses, Gaussian apertures, cascaded paraxial systems, and systems having quadratic amplitude as well as phase variations about the axis. By following a coordinate-free approach, rather than proposing solutions in a particular coordinate system, it was possible to derive an elegant and closed-form expression for the electromagnetic field, the vector angular spectrum, and the Poynting vector at the output plane of the ABCD system. It is found that the gVHzG beams are a class of vector fields which exhibit the property of form-invariance under paraxial optical transformations. The formulation described in this paper can be useful in applications where the polarization of the fields is of major concern [5, 6, 13, 14, 15].

2. Propagation of the generalized vector HzG beams

Consider an electromagnetic paraxial beam with time dependence $\exp(-i\omega t)$ travelling in the z direction (unit vector $\widehat{\mathbf{z}}$) through an ABCD axisymmetric optical system with input and output planes located at $z = z_1$ and $z = z_2$, respectively. The system is characterized by an ABCD

#73591 - $15.00 USD Received 2 August 2006; revised 15 September 2006; accepted 15 September 2006

matrix with, in general, complex elements A, B, C, and D that satisfy the unimodular relation $AD-BC=1$.

Let us express both the position vector $\mathbf{R}$ and the wave vector $\mathbf{K}$ as

$$\mathbf{R}=(\mathbf{r},z)\,,\qquad \mathbf{r}=(x,y)=(r,\theta)\,;\qquad \mathbf{K}=(\mathbf{k},k_z)\,,\qquad \mathbf{k}=(k_x,k_y)=(k,\phi), \tag{1}$$

where $\mathbf{r}$ and $\mathbf{k}$ are the positions at the transverse planes of the configuration and frequency spaces, respectively. Additionally, we will denote a general vector field as $\mathbf{F}=\mathbf{f}+f_z\widehat{\mathbf{z}}$, where $\mathbf{f}=(f_x,f_y)$ represents the transverse part of the field. The transverse nabla operators in the configuration and frequency spaces are denoted by $\nabla=\widehat{\mathbf{x}}\partial/\partial x+\widehat{\mathbf{y}}\partial/\partial y$ and $\widetilde{\nabla}=\widehat{\mathbf{k}}_x\partial/\partial k_x+\widehat{\mathbf{k}}_y\partial/\partial k_y$, respectively.

Throughout the paper, the suffixes "1" and "2" denote the evaluation of the respective physical quantity (or operator) at the input ($z=z_1$) and output ($z=z_2$) transverse planes of the ABCD system.

2.1. Definition of the generalized vector HzG beams

We commence the analysis by defining the transverse electric $\mathbf{e}(\mathbf{r})$ and magnetic $\mathbf{h}(\mathbf{r})$ vectors of a first-class (TM) gVHzG beam at the input plane of the ABCD system as [8]

$$\mathbf{e}_1(\mathbf{r}_1)=\exp\left(\frac{iKr_1^2}{2q_1}\right)\nabla_1 W(\mathbf{r}_1;\kappa_1),\qquad \mathbf{h}_1(\mathbf{r}_1)=\left(\frac{\varepsilon}{\mu}\right)^{1/2}\widehat{\mathbf{z}}\times\mathbf{e}_1(\mathbf{r}_1), \tag{2}$$

where $K=|\mathbf{K}|=\omega(\mu\varepsilon)^{1/2}$ is the wave number.

The electric vector field in Eqs. (2) results from the product of two functions, each depending on one parameter. First, the Gaussian modulation is characterized by a complex beam parameter $q_1=q_1^{\mathscr{R}}+iq_1^{\mathscr{I}}$, where the superscripts $\mathscr{R}$ and $\mathscr{I}$ denote the real and imaginary parts of a complex quantity, respectively. For simplicity in dealing with the ABCD system, the parameter q_1 is used throughout the paper. The physical meaning of q_1 is contained in the known relation $1/q_1=1/\mathfrak{R}_1+i2/Kw_1^2$, where $\mathfrak{R}_1$ is the radius of curvature of the phase fronts, and w_1 is the $1/e$ amplitude spot size of the Gaussian modulation. In assuming a complex q_1 we are allowing for the possibility that the Gaussian apodization has an initial converging ($q_1^{\mathscr{R}}<0$) or diverging ($q_1^{\mathscr{R}}>0$) spherical wavefront. Additionally, the condition $q_1^{\mathscr{I}}<0$ must be fulfilled in order to satisfy the physical requirement that the field amplitude vanishes as r becomes arbitrarily large.

The gradient $\nabla_1 W(\mathbf{r}_1;\kappa_1)$ in Eq. (2) provides the vector nature of the transverse electric field. The scalar function $W(\mathbf{r}_1;\kappa_1)$ is a solution of the two-dimensional Helmholtz equation $\left[\nabla_1^2+\kappa_1^2\right]W=0$, and physically describes the transverse shape of an ideal scalar nondiffracting beam [16, 22, 23]. Since a vector beam $\mathbf{e}_1(\mathbf{r}_1)$ is determined from a scalar function $W(\mathbf{r}_1;\kappa_1)$, throughout the paper we will refer to the latter as the *seed* function. The function W can be formally expanded in terms of plane waves as

$$W(\mathbf{r}_1;\kappa_1)=\int_{-\pi}^{\pi} g(\phi)\exp\left[i\kappa_1\left(x_1\cos\phi+y_1\sin\phi\right)\right]\mathrm{d}\phi, \tag{3}$$

where κ_1 and $g(\phi)$ are the transverse wave number and the angular spectrum of the ideal scalar nondiffracting beam, respectively. Since $g(\phi)$ is arbitrary, an infinite number of profiles can be obtained, see section 2.6 for important special cases.

The fields in Eq. (2) are purely transverse and correspond to the zeroth-order electric and magnetic fields of the perturbative series expansion of the Maxwell equations provided by Lax *et al.* [1]. The Lax expansion also showed that in next-order correction small longitudinal field components must be present, and their values are obtained from the transverse components

#73591 - $15.00 USD Received 2 August 2006; revised 15 September 2006; accepted 15 September 2006

through

$$e_{z,1} = \frac{i}{K}\nabla_1 \cdot \mathbf{e}_1 = -\exp\left(\frac{iKr_1^2}{2q_1}\right)\left(\frac{i\kappa_1^2}{K}W + \nabla_1 W \cdot \frac{\mathbf{r}_1}{q_1}\right), \tag{4a}$$

$$h_{z,1} = \frac{i}{K}\nabla_1 \cdot \mathbf{h}_1 = -\sqrt{\frac{\varepsilon}{\mu}}\exp\left(\frac{iKr_1^2}{2q_1}\right)(\widehat{\mathbf{z}} \times \nabla_1 W) \cdot \frac{\mathbf{r}_1}{q_1}. \tag{4b}$$

TE polarized gVHzG beams: For the sake of space, throughout the paper we shall deal with the explicit expressions for the TM beams. However second-class (TE) beams can be readily obtained from Eqs (2) by applying the duality property, i.e. replacing $\mathbf{E}$ with $(\mu/\varepsilon)^{1/2}\mathbf{H}$ and $(\mu/\varepsilon)^{1/2}\mathbf{H}$ with $-\mathbf{E}$, namely

$$\mathbf{e}_1^{(TE)}(\mathbf{r}_1) = -\exp\left(\frac{iKr_1^2}{2q_1}\right)[\widehat{\mathbf{z}} \times \nabla_1 W], \qquad \mathbf{h}_1^{(TE)}(\mathbf{r}_1) = \sqrt{\frac{\varepsilon}{\mu}}\exp\left(\frac{iKr_1^2}{2q_1}\right)\nabla_1 W. \tag{5}$$

The corresponding longitudinal components are obtained by applying the divergence operator as shown in Eqs. (4).

2.2. Classification of the generalized vector HzG beams

In the theory of nondiffracting beams, the parameter κ_1 in Eq. (3) is customarily assumed to be real and positive [16, 22, 23]. For the sake of generality, we will let $\kappa_1 = \kappa_1^{\mathscr{R}} + i\kappa_1^{\mathscr{I}}$ be arbitrarily complex allowing the possibility of having three kinds of beams:

- *Ordinary* VHzG (oVHzG) beams correspond to purely real $\kappa_1 = \kappa_1^{\mathscr{R}}$ for which the seed function $W(\mathbf{r}_1;\kappa_1)$ is a two-dimensional purely oscillatory (or standing wave) function. The physical meaning of $\kappa_1^{\mathscr{R}}$ is clear, as it governs the oscillatory behavior of the function W in the transverse direction. Far from the z axis, the spatial period of the field oscillations tends monotonically to $2\pi/\kappa_1^{\mathscr{R}}$. The special case when $\kappa_1^{\mathscr{R}} > 0$ and $q_1 = -iKw_1^2/2$ is purely imaginary leads to the ordinary vector solutions discussed in Ref. [8], where w_1 is the standard $1/e$ amplitude spot size of the Gaussian apodization.
- *Modified* VHzG (mVHzG) beams correspond to purely imaginary $\kappa_1 = i\kappa_1^{\mathscr{I}}$. In this case $W\left(\mathbf{r}_1, \kappa_1^{\mathscr{I}}\right)$ is an evanescent seed function which satisfies the modified Helmholtz equation $\left[\nabla_1^2 - \left(\kappa_1^{\mathscr{I}}\right)^2\right]W = 0$. Two concrete examples of seed functions of the modified kind are provided by the cosh-Gaussian beams [17] and the modified Bessel beams [18, 19].
- *Generalized* VHzG (gVHzG) beams correspond to the general case when κ_1 is complex. As we will see, the gVHzG can be interpreted as intermediate solutions between oVHzG and mVHzG beams.

In order that fields in Eq. (2) satisfy the paraxial approximation, it is needed that $K \gg 1/w_1$, i.e. the Gaussian spot width is many wavelengths wide, and additionally that $K \gg |\kappa_1|$, i.e. the spatial transverse beam oscillations must be many wavelengths wide. Two limiting cases of the gVHzG beams are of particular interest: (a) pure vector nondiffracting beams are obtained when $\left|q_1^{\mathscr{I}}\right| \to \infty$, and (b) the special value $\kappa_1 = 0$ leads to the generalized vector Laplace-Gauss beams, for which the seed function W is now a solution of the 2D Laplace equation [8].

2.3. Propagation of the electromagnetic field through the ABCD system

Paraxial propagation of the electric vector field $\mathbf{e}_1(\mathbf{r}_1)$ through the ABCD system can be performed by solving the Huygens diffraction integral [20, 21]

$$\mathbf{e}_2(\mathbf{r}_2) = \frac{K\exp(iKL_0)}{i2\pi B}\iint_{-\infty}^{\infty}\mathbf{e}_1(\mathbf{r}_1)\exp\left[\frac{iK}{2B}\left(Ar_1^2 - 2\mathbf{r}_1\cdot\mathbf{r}_2 + Dr_2^2\right)\right]\mathrm{d}^2\mathbf{r}_1, \tag{6}$$

#73591 - $15.00 USD Received 2 August 2006; revised 15 September 2006; accepted 15 September 2006

where $\mathbf{e}_2(\mathbf{r}_2)$ is the output transverse electric field, and L_0 is the optical path length from the input to the output plane of the ABCD system measured along the optical axis. The vector integral in Eq. (6) can be treated as a pair of independent scalar integrals by decomposing the transverse vector $\mathbf{e}_1(\mathbf{r}_1)$ into orthogonal linearly polarized parts. After substituting each Cartesian component of Eq. (2) and the expansion given by Eq. (3) into Eq. (6), the integration can be performed applying the changes of variables $x_j = u_j \cos\phi - v_j \sin\phi$, and $y_j = u_j \sin\phi + v_j \cos\phi$, for $j = 1,2$. Upon returning to the original variables and regrouping the Cartesian components into a vector function, we obtain (see the detailed derivation in the appendix A)

$$\mathbf{e}_2(\mathbf{r}_2) = \frac{\kappa_1}{\kappa_2} \exp\left(-i\frac{\kappa_1\kappa_2 B}{2K}\right) G(\mathbf{r}_2, q_2) \nabla_2 W(\mathbf{r}_2; \kappa_2), \tag{7a}$$

$$\mathbf{h}_2(\mathbf{r}_2) = \left(\frac{\varepsilon}{\mu}\right)^{1/2} \widehat{\mathbf{z}} \times \mathbf{e}_2(\mathbf{r}_2), \tag{7b}$$

where

$$G(\mathbf{r}_2, q_2) = \frac{\exp(iKL_0)}{A + B/q_1} \exp\left(\frac{iKr_2^2}{2q_2}\right), \tag{8}$$

is the output field of a scalar Gaussian beam with input parameter q_1 travelling axially through the ABCD system, and the transformation laws for the parameters q_1 and κ_1 from the plane z_1 to the plane z_2 are

$$q_2 = \frac{Aq_1 + B}{Cq_1 + D}, \qquad \kappa_2 = \frac{\kappa_1 q_1}{Aq_1 + B}. \tag{9}$$

Equations (7) are the main result of this paper, they permit an arbitrary gVHzG beam to be propagated in closed-form through an axisymmetric ABCD optical system with real or complex matrix elements. The presence of the fundamental Gaussian beam $G(\mathbf{r}_2, q_2)$ in Eq. (7a) provides the confinement mechanism which ensures the transverse intensity distribution vanishes at large values of r, and that the beam is square integrable. As expected, Eqs. (7) reduces to Eq. (2) when the ABCD matrix becomes the identity matrix.

Like the input field [Eqs. (4)], the longitudinal components of the electric $e_{z,2}$ and the magnetic $h_{z,2}$ fields at the output plane can be readily obtained by applying the operator $[(i/K)\nabla_2 \cdot]$ over the corresponding transverse components $\mathbf{e}_2(\mathbf{r}_2)$ and $\mathbf{h}_2(\mathbf{r}_2)$, respectively.

2.4. Poynting vector of the generalized vector HzG beams

The time-averaged Poynting vector is given by $\langle \mathbf{S} \rangle = \mathrm{Re}\,(\mathbf{E} \times \mathbf{H}^*)/2$. It can be decomposed as $\langle \mathbf{S} \rangle = \langle s_z \rangle \widehat{\mathbf{z}} + \langle \mathbf{s} \rangle$, where $\langle s_z \rangle$ is the longitudinal part which determines the flow of energy in the direction of propagation z, and $\langle \mathbf{s} \rangle$ is the transverse part which determines the flow of energy perpendicular to this direction. The Poynting vector can be calculated at the input $(j = 1)$ and output $(j = 2)$ planes using the corresponding expressions for the electric and magnetic fields, we have

$$\langle \mathbf{S}_j \rangle = \frac{1}{2}\left(\frac{\varepsilon}{\mu}\right)^{1/2} |f_j|^2 \left\{ |\nabla_j W|^2 \widehat{\mathbf{z}} + \mathrm{Re}\left[\left(\frac{i\kappa_j^2}{K} W + \nabla_j W \cdot \frac{\mathbf{r}_j}{q_j} \right) \nabla_j W^* \right] \right\}, \tag{10}$$

where $f_1 = \exp\left(iKr_1^2/2q_1\right)$, and $f_2 = (\kappa_1/\kappa_2)\exp(-i\kappa_1\kappa_2 B/2K)\, G(\mathbf{r}_2, q_2)$.

From Eq. (10) we note that the energy flux density along the longitudinal direction is proportional to the squared magnitude of the transverse electric field vector. Since W and q_j are, in general, complex, the beam exhibits a transverse flow of energy whose radial part is a manifestation of diffraction. For a paraxial beam it is expected that the longitudinal part of the energy flux be much more significant than the transverse part, in fact a simple analysis of orders of

#73591 - $15.00 USD Received 2 August 2006; revised 15 September 2006; accepted 15 September 2006

magnitude in Eq. (10) reveals that the longitudinal flow is at least Kw_1 times the transverse one. Finally, for a lossless medium, the light power carried by the beam in longitudinal direction $\iint \langle \mathbf{S}_j \rangle \cdot \widehat{\mathbf{z}}\, \mathrm{d}^2\mathbf{r}_j$ remains constant for any z plane.

2.5. *Propagation of the vector angular spectrum*

The electric field $\mathbf{e}(\mathbf{r})$ of the gVHzG beam at either the input or output planes of the ABCD system admits the plane wave expansion of the form $\mathbf{e}(\mathbf{r}) = (1/2\pi) \iint_{-\infty}^{\infty} \widetilde{\mathbf{e}}(\mathbf{k}) \exp(i\mathbf{k}\cdot\mathbf{r})\, \mathrm{d}^2\mathbf{k}$, where $\widetilde{\mathbf{e}}(\mathbf{k})$ is the vector angular spectrum whose functional form is obtained by Fourier inversion

$$\widetilde{\mathbf{e}}(\mathbf{k}) = \frac{1}{2\pi} \iint_{-\infty}^{\infty} \mathbf{e}(\mathbf{r}) \exp(-i\mathbf{k}\cdot\mathbf{r})\, \mathrm{d}^2\mathbf{r}. \tag{11}$$

After inserting Eqs. (2) and (7a) into Eq.(11) and performing the integrals we obtain the vector angular spectra at the input and output planes of the ABCD system, namely

$$\widetilde{\mathbf{e}}_1(\mathbf{k}_1) = i \exp\left(-i\frac{q_1\kappa_1^2}{2K}\right) \exp\left(-i\frac{q_1 k_1^2}{2K}\right) \widetilde{\nabla}_1 W\left(\mathbf{k}_1; \frac{q_1\kappa_1}{K}\right), \tag{12a}$$

$$\widetilde{\mathbf{e}}_2(\mathbf{k}_2) = \frac{\kappa_1 K}{\kappa_2 q_2} \exp\left(-i\frac{q_2\kappa_2^2 + \kappa_1\kappa_2 B}{2K}\right) \widetilde{G}(\mathbf{k}_2, q_2) \widetilde{\nabla}_2 W\left(\mathbf{k}_2; \frac{B\kappa_2^2}{K\kappa_1}\right), \tag{12b}$$

where $\widetilde{\nabla} = \widehat{\mathbf{k}}_x \partial/\partial k_x + \widehat{\mathbf{k}}_y \partial/\partial k_y$ is the transverse nabla operator in the $\mathbf{K}$ space, and

$$\widetilde{G}(\mathbf{k}_2, q_2) = \left(\frac{iq_2}{K}\right) \frac{\exp(iKL_0)}{A + B/q_1} \exp\left(-i\frac{q_2 k_2^2}{2K}\right) \tag{13}$$

is the Fourier transform of the Gaussian function $G(\mathbf{r}_2, q_2)$ in Eq. (8).

2.6. *Remarks on the coordinates systems and polarization basis*

The electromagnetic fields in Eqs. (2), (7) and (12) are completely general in the sense that they do not depend on a particular coordinate system. The vector beam solutions are constructed starting from scalar solutions of the 2D Helmholtz equation which can be formally expanded in terms of plane waves according to Eq. (3). Although this integral expansion constitute a general integral solution, it is important to note that the 2D Helmholtz equation can also be solved in several orthogonal coordinate systems using the separation of variables method [11, 24, 25]. This fact leads to have complete and orthogonal families of eigenfunctions of the 2D Helmholtz equation.

Of particular interest are the families of eigenfunctions of the 2D Helmholtz equation expressed in Cartesian, polar, elliptic, and parabolic coordinates [11]. For Cartesian coordinates (x,y), generalized vector Gaussian beams can be constructed from superpositions of fundamental plane waves of the form $W = \exp(i\overrightarrow{\kappa}_1 \cdot \mathbf{r}_1) = \exp[i\kappa_1(x\cos\phi + y\sin\phi)]$, see, for example, the cosine-Gauss beams studied in Ref. [11]. The case of the polar coordinates (r,θ) corresponds to eigenfunctions $W = J_m(\kappa r)\exp(im\theta)$ for which gVHzG beams reduce to the mth-order generalized vector Bessel-Gauss beams [4]. For elliptic coordinates (ξ,η), generalized vector even Mathieu-Gauss beams of mth-order and ellipticity parameter ε can be constructed from the eigenfunctions $W = \mathrm{Je}_m(\xi,\varepsilon)\mathrm{ce}_m(\eta,\varepsilon)$, where $\mathrm{Je}(\cdot)$ and $\mathrm{ce}(\cdot)$ are the radial and angular even Mathieu functions of mth-order and parameter ε, respectively [22]. For parabolic coordinates (u,v), generalized vector even parabolic-Gauss beams can be constructed from the eigenfunctions $W = \mathrm{Pe}\left(u\sqrt{2\kappa}; p\right) \mathrm{Pe}\left(v\sqrt{2\kappa}; -p\right)$, where $\mathrm{Pe}(\cdot)$ is a parabolic cylinder function of parameter p and even parity [23].

#73591 - $15.00 USD Received 2 August 2006; revised 15 September 2006; accepted 15 September 2006

On the other hand, the gradient operator in Eqs. (2) and (7a) can also be expressed in several coordinate systems [24, 25], with the consequence that several polarization basis may be used to decompose the field vector $\mathbf{e}_2(\mathbf{r}_2)$ at any point $\mathbf{r}_2$ into two orthogonal polarized transverse parts. For instance, in polar coordinates, the transverse vector fields can be split into radial and azimuthal polarized components, or in elliptic coordinates, into elliptic and hyperbolic polarized components. Explicit expressions for these polarization basis associated to particular coordinate systems can be found elsewhere [24, 25].

It is important to emphasize that a general vector beam solution is found by the superposition of TM and TE vector modes, i.e.

$$\mathbf{E} = \alpha \mathbf{E}^{(TM)} + \beta \mathbf{E}^{(TE)}, \tag{14}$$

where α and β are arbitrary constants. By combining the different polarization basis with the different seed functions $W(\mathbf{r}_2;\kappa_2)$ a large variety of beam profiles with specific polarization states could be constructed through superposition. As example, consider the basis of circular polarizations $\widehat{\mathbf{u}}^{\pm} = (\widehat{\mathbf{x}} \pm i\widehat{\mathbf{y}})/\sqrt{2}$. It is easy to verify that the gradient of W in Eqs. (2) and (7a) can be expressed in the basis of vectors $\widehat{\mathbf{u}}^{\pm}$ as

$$\nabla W = \frac{1}{\sqrt{2}}\left(\frac{\partial W}{\partial x} - i\frac{\partial W}{\partial y}\right)\widehat{\mathbf{u}}^{+} + \frac{1}{\sqrt{2}}\left(\frac{\partial W}{\partial x} + i\frac{\partial W}{\partial y}\right)\widehat{\mathbf{u}}^{-}. \tag{15}$$

Now, gVHzG beams with pure left $(+)$ and right $(-)$ circularly polarized beams can be constructed from Eq. (15) using the superposition $\mathbf{e}^{\pm} = \mathbf{e}^{(TM)} \pm i\mathbf{e}^{(TE)}$ at either the input ($j = 1$) or output ($j = 2$) planes of the ABCD system, we have explicitly

$$\mathbf{e}_j^{\pm}(\mathbf{r}_j) = \sqrt{2} f_j \left(\frac{\partial W}{\partial x_j} \mp i\frac{\partial W}{\partial y_j}\right)\widehat{\mathbf{u}}^{\pm}, \tag{16}$$

where $f_1 = \exp\left(iKr_1^2/2q_1\right)$, and $f_2 = (\kappa_1/\kappa_2)\exp\left(-i\kappa_1\kappa_2 B/2K\right)G(\mathbf{r}_2, q_2)$. A similar approach can be applied for the vector angular spectra in Eq. (12) to derive the corresponding circular polarization states.

Finally, from Eqs. (2) and (5), it is clear that the polarization of the transverse electric field of the TM and TE beams is defined entirely by the operations ∇W and $\widehat{\mathbf{z}} \times \nabla W$, respectively. Both vector fields $\Psi^{(1)} = \nabla W$ and $\Psi^{(2)} = \widehat{\mathbf{z}} \times \nabla W$ constitute two independent vector solutions of the 2D vector Helmholtz equation $\nabla^2\Psi + \kappa^2\Psi = 0$ [24, 25]. Now, if we set the function $W = W_m$ to be the m-th eigensolution belonging to a countable set of complete and orthogonal solutions of the scalar Helmholtz equation, then, because of the linearity and the one-to-one mapping of the gradient operator, the properties of linear independence, orthogonality, and completeness exhibited by the family of scalar solutions W_m are transferred to the corresponding families of vector fields $\Psi^{(1)}$ and $\Psi^{(2)}$. Additionally, the transverse fields of a TM and a TE beams are orthogonal, even when their seed functions W_m are equal. In this sense, the gVHzG beams exhibit similar polarization properties than the ideal vector nondiffracting beams [3, 7, 16] and waveguides with constant cross-section [9, 10, 24].

3. Physical discussion of the propagation properties

In Section 2 we have demonstrated that localized vector beam solutions of the Maxwell equations can be propagated through an ABCD optical system in a closed and coordinate-free form. Particular attention was focused on the propagation of the vector beams and their vector angular spectra. Several considerations for the coordinate system and polarization basis were also discussed. To get involved in the propagation details of the gVHzG beams, let us study in this section two very illustrative examples.

#73591 - $15.00 USD Received 2 August 2006; revised 15 September 2006; accepted 15 September 2006

3.1. *Free space propagation*

We consider first the free space propagation along a distance $L = z_2 - z_1$. The input and output fields are given by Eqs. (2) and (7a) with $A = 1$, $B = L$, $C = 0$, and $D = 1$. From Eqs. (9) the transformation laws become

$$q_2 = q_1 + L, \qquad \kappa_2 = \frac{\kappa_1 q_1}{q_1 + L}, \tag{17}$$

where we note that the product $q_2\kappa_2 = q_1\kappa_1$ remains constant under free-space propagation.

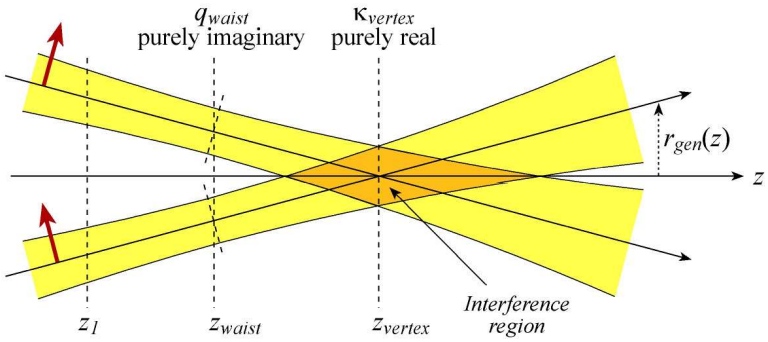

Fig. 1. Physical picture of the decomposition of a gVHzG beam propagating in free space in terms of fundamental vector Gaussian beams whose mean propagation axes lie on the surface of a double cone.

In a similar fashion to the scalar HzG beams [11], to gain a basic understanding of the features of the gVHzG beams propagating in free space, one may consider that a gVHzG beam is formed as a superposition of fundamental vector Gaussian beams (see Fig. 1) whose mean propagation axes lie on the surface of a double cone, whose amplitudes are modulated angularly by the function $g(\phi)$. This physical picture is evident after replacing Eqs. (17) into Eq. (7a) and observing that the TM polarized gVHzG beams in vacuum can be rewritten as

$$\mathbf{e}_2(\mathbf{r}_2) = \int_{-\pi}^{\pi} g(\phi)\mathbf{g}_2(\mathbf{r}_2;\phi)\mathrm{d}\phi, \tag{18}$$

where

$$\mathbf{g}_2(\mathbf{r}_2;\phi) = i\exp\left(-i\frac{\kappa_1^2}{2K}\frac{L}{\zeta}\right)\frac{\exp(iKL)}{\zeta}\exp\left(\frac{iKr_2^2}{2q_1\zeta}\right)\exp\left(i\frac{\overrightarrow{\kappa}_1\cdot\mathbf{r}_2}{\zeta}\right)\overrightarrow{\kappa}_1, \tag{19}$$

with $\zeta \equiv 1 + L/q_1$ and $\overrightarrow{\kappa}_1 = \kappa_1(\cos\phi\hat{\mathbf{x}} + \sin\phi\hat{\mathbf{y}})$ Equation (19) represents the free space propagation along a distance L of a tilted Gaussian beam with input parameter q_1 whose mean wave vector has a projection $\overrightarrow{\kappa}_1$ over the transverse plane [11], and whose polarization vector points in direction of the vector $\overrightarrow{\kappa}_1$.

The generatrix of the double cone shown in Fig. 1 corresponds to the linear propagation of the centroid of the individual Gaussian beams, and from Eqs. (7a) it is found to be

$$r_{gen}(z) = \frac{|q_1|^2\kappa_1^{\mathscr{I}}}{Kq_1^{\mathscr{I}}} + \frac{\kappa_1^{\mathscr{R}}q_1^{\mathscr{I}} + \kappa_1^{\mathscr{I}}q_1^{\mathscr{R}}}{Kq_1^{\mathscr{I}}}(z - z_1). \tag{20}$$

In Fig. 1 we identify three important transverse planes:

- The *initial plane* at $z = z_1$.

#73591 - $15.00 USD Received 2 August 2006; revised 15 September 2006; accepted 15 September 2006

- The *waist plane* ($z = z_{waist}$) corresponds to the plane where the width of the elementary Gaussian beams is minimum, i.e. where the radial factor $\exp\left(iKr_2^2/2q_2\right)$ becomes a real Gaussian envelope. Using this condition, from Eqs. (17) we get $z_{waist} = z_1 - q_1^{\mathscr{R}}$. At the waist plane the parameter q becomes purely imaginary $q_{waist} = iq_1^{\mathscr{I}}$, whereas the parameter κ reduces to $\kappa_{waist} = \kappa_1\left(1 - iq_1^{\mathscr{R}}/q_1^{\mathscr{I}}\right)$. From the general expression of the Poynting vector Eq. (10) we note that if W and κ is set to be purely real, then at the waist plane the energy flow becomes purely longitudinal.

- The *vertex plane* ($z = z_{vertex}$) corresponds to the plane where the main propagation axes of the constituent Gaussian beams intersect. As shown in Fig. 1, the pseudo-nondiffracting region delimits the region where significant interference of the constituent vector Gaussian beams occurs, and where the transverse beam profile exhibits a standing-wave behavior. The evaluation of the condition $r_{gen} = 0$ in Eq. (20) yields

$$z_{vertex} = z_1 - \frac{|q_1|^2\,\kappa_1^{\mathscr{I}}}{\kappa_1^{\mathscr{R}} q_1^{\mathscr{I}} + \kappa_1^{\mathscr{I}} q_1^{\mathscr{R}}}. \tag{21}$$

  Note that at the vertex plane the parameter κ becomes purely real $\kappa_{vertex} = \kappa_1^{\mathscr{R}} + \kappa_1^{\mathscr{I}} q_1^{\mathscr{R}}/q_1^{\mathscr{I}}$, with the consequence that at this plane the beam profile belongs to the oVHzG kind with $q_{vertex} = \kappa_1 q_1/\kappa_{vertex}$. At the vertex plane the extent of the pseudo-nondiffracting region is maximum, and its $1/e$ amplitude Gaussian spot size can be calculated with $w_{vertex} = \left[K\,\mathrm{Im}\left(1/q_{vertex}\right)/2\right]^{-1/2}$.

In general, the initial, the waist, and the vertex planes are located at different axial positions, as shown in Fig. 1. The ordinary VHzG beams studied in Ref. [8] constitute the special case when $z_1 = 0$, $q_1^{\mathscr{R}} = 0$, and $\kappa_1^{\mathscr{I}} = 0$, for which the three planes coincide at $z = 0$, and the cone generatrix reduces to the expected $r_{gen} = \left(\kappa_1^{\mathscr{R}}/K\right) z$.

On the other side, the mVHzG beams occur when $\kappa_1^{\mathscr{R}} = 0$; if we additionally set $q_1^{\mathscr{R}} = 0$ then $r_{gen} = r_0 = q_1^{\mathscr{I}}\,\kappa_1^{\mathscr{I}}/K$ becomes a constant, and therefore the mVHzG beams may be viewed as a superposition of vector Gaussian beams whose axes are parallel to the z axis and lie on the surface of a circular cylinder of radius r_0.

Finally, we remark that the transverse fields of the gVHzG beams propagating in free space satisfy the paraxial wave equation $\left[\nabla_1^2 + i2K\partial/\partial z\right]\{\mathbf{e}_1, \mathbf{h}_1\} = 0$ and correspond to the purely transverse zeroth-order electric and magnetic fields of the perturbative series expansion of the Maxwell equations provided by Lax *et al.* [1].

3.2. Propagation through a GRIN medium

Let us consider now the propagation of the gVHzG beams through a graded refractive-index (GRIN) medium with quadratic index variation $n(r) = n_0(1 - r^2/2a^2)$. The ABCD transfer matrix from plane z_1 to plane $z_2 = z_1 + L$ is given by

$$\begin{bmatrix} A & B \\ C & D \end{bmatrix} = \begin{bmatrix} \cos(L/a) & a\sin(L/a) \\ -\sin(L/a)/a & \cos(L/a) \end{bmatrix}. \tag{22}$$

For a general input vector field of the form (2), the propagated vector field at a distance z_2 is described by Eq. (7a). Substitution of the matrix elements in Eq. (22) into Eqs. (9) yields the parameter transformations:

$$q_2 = a\frac{q_1\cos(L/a) + a\sin(L/a)}{-q_1\sin(L/a) + a\cos(L/a)}, \qquad \kappa_2 = \frac{\kappa_1 q_1}{q_1\cos(L/a) + a\sin(L/a)}, \tag{23}$$

#73591 - $15.00 USD Received 2 August 2006; revised 15 September 2006; accepted 15 September 2006

where we note that, under propagation, the parameters q and κ vary periodically with a longitudinal period $2\pi a$, therefore, the initial field distribution self-reproduces after a distance $2\pi a$.

To show the role played by the gVHzG beams as intermediate vector solutions between oVHzG and mVHzG beams, let us assume that the input field at $z_1 = 0$ belongs to the oVHzG kind (i.e. $\kappa_1^{\mathscr{I}} = 0$) with an initial real Gaussian apodization of width w_1 (i.e. $q_1 = iq_1^{\mathscr{I}} = -iKw_1^2/2$). For a propagation distance $L = L_F = \pi a/2$, the ABCD matrix Eq. (22) reduces to $[0, a; -1/a, 0]$ which is indeed identical to the matrix transformation from the first to the second focal plane of a converging thin lens of focal length a, i.e. a Fourier transformer. At the Fourier plane $L = L_F$, from Eqs. (23) we see that both parameters $q_2 = ia^2/q_1^{\mathscr{I}}$ and $\kappa_2 = i\kappa_1^{\mathscr{R}} q_1^{\mathscr{I}}/a$ become purely imaginary. It is now evident that if an oVHzG profile is Fourier transformed, a mVHzG profile will be obtained, and vice versa. The intermediate profiles belong to the gVHzG kind where, for the particular case of the GRIN medium, the transition between both types of beams is characterized by the continuous transformations given in Eqs. (23).

The special case when the parameter a of the GRIN medium is equal to the Rayleigh distance (i.e. $z_R = Kw_1^2/2$) of the initial Gaussian apodization is of particular interest. From Eqs. (23) we see that the Gaussian width $q_2 = q_1 = -ia$ remains constant under propagation and that the wave number $\kappa_2 = \kappa_1 \exp(-iL/a)$ rotates at a constant rate over the complex plane $\left(\kappa_2^{\mathscr{R}}, \kappa_2^{\mathscr{I}}\right)$ as the beam propagates through the GRIN medium. For brevity, we will refer to the case when $a = Kw_1^2/2$ as a *balanced* propagation, and a *non-balanced* otherwise.

In Figs. 2 and 3 we show the propagation of the transverse intensity distribution and the electric vector field for several circularly polarized gVHzG beams with $\kappa_1 = 30\ \mathrm{mm}^{-1}$ through a GRIN medium with $a = 1/\sqrt{2}\pi$ m. The input fields are given by Eq. (16) with $j = 1$ for $K = 2\pi/\lambda$ and $\lambda = 632.8$ nm. The animations were constructed by calculating the field at 200 transverse planes evenly spaced from the input ($z_1 = 0$) to the output ($z_2 = 4L_F = 2\pi a$) planes using Eq. (16) with $j = 2$ to generate the left or right circularly polarized fields as the case may be.

The fields shown in Fig. 2 correspond to a seed function $W(\mathbf{r}_1)$ given by the superposition of N plane waves of the general form

$$W(\mathbf{r}_1) = \sum_{n=1}^{N} A_n \exp\left[i\kappa_1 r_1 \cos(\theta_1 - \phi_n)\right], \tag{24}$$

where A_n are complex amplitudes. For Fig. 2(a) we have chosen a left circularly polarized oVHzG beam in a balanced condition ($q_1 = -ia = -i/\sqrt{2}\pi$) with $N = 3$, $A_n = \{1, 1, 1\}$, and $\phi_n = \{90^\circ, -30^\circ, -150^\circ\}$. Note that the width of the constituent Gaussian beams remains constant under propagation because the beams are balanced. Following the established convention, at a given z plane, the transverse components of the fields rotate anti-clockwise for left-handed circular polarization as time increases. The field at the plane $z_2 = L_F$ is shown Fig. 2(b), where we note that for the selected amplitudes $A_n = 1$ the beam polarization becomes purely radial. To show the non-balanced condition, in Fig. 2(c) we propagated the same gVHzG by setting now $q_1 = 0.4 - i0.8/\sqrt{2}\pi$ and keeping all remaining parameters unchanged. The video shows clearly that the width of the constituent Gaussian beams change under propagation and reach a minimum at the plane where q_2 in Eqs. (23) becomes purely imaginary ($\sim 1.22L_F$)

In Fig. 2(e) we show a right circularly polarized balanced oVHzG beam constructed with $N = 8$ constituent Gaussian beams. By means of the amplitudes and phases of the coefficients A_n it is possible to adjust the polarization state of the resulting beam. In this case we set $A_n = i$ such that the electric field at the plane $z_2 = L_F$ now becomes purely azimuthal, as shown in Fig. 2(f). In Fig. 2(g) we set $A_n = \exp(-i\pi n/4)$ such that the electric field vectors at each point on the plane $z_2 = L_F$ become parallel, as shown in Fig. 2(h).

Figures 3(a) to 3(d) show the vector propagation of ordinary vector Bessel-Gauss (VBG)

#73591 - $15.00 USD Received 2 August 2006; revised 15 September 2006; accepted 15 September 2006

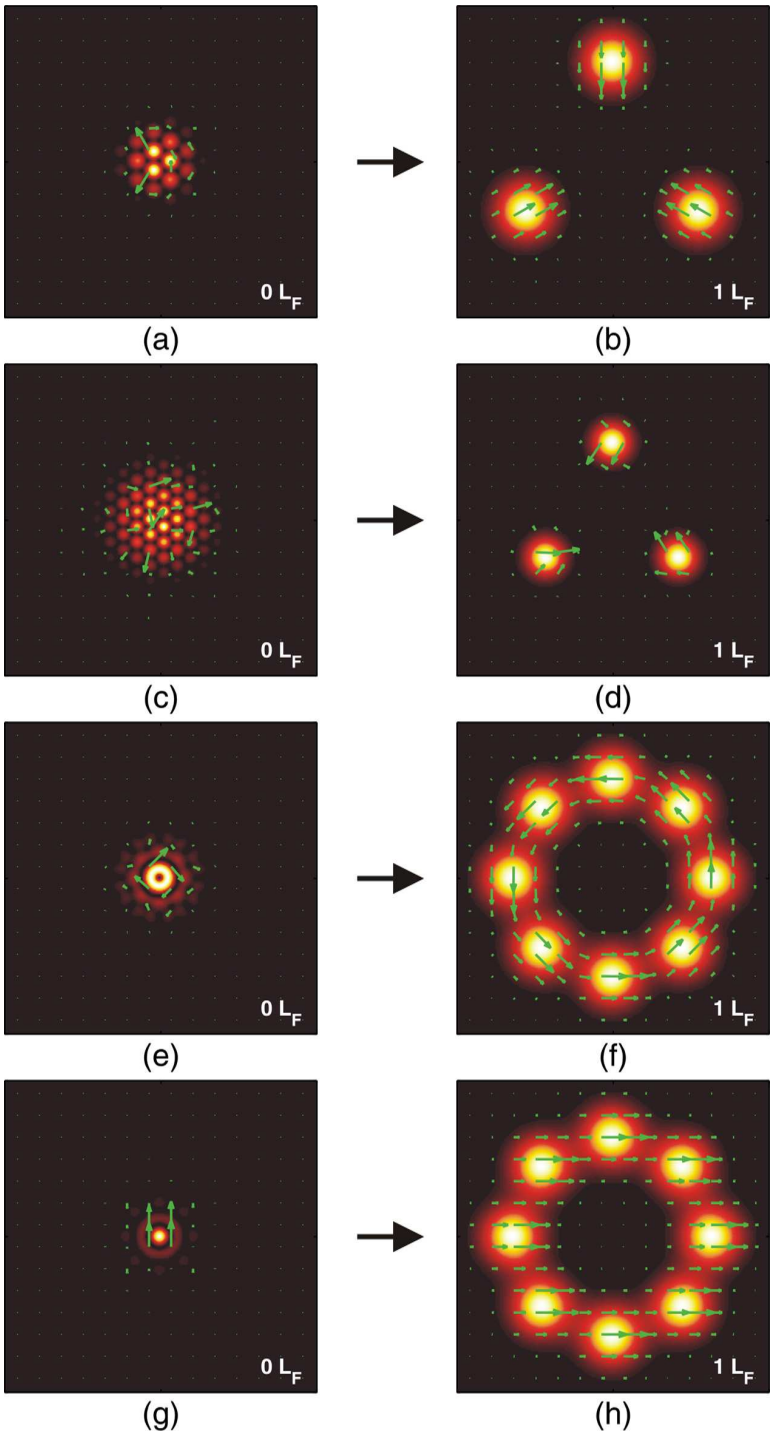

Fig. 2. Propagation of the transverse intensity distribution and the electric vector field for circularly polarized gVHzG beams constructed with finite superposition of vector Gaussian beams. The parameter data for the propagations are included within the text. The movies show the evolution from $z = 0$ to $z = 4L_F$. (Movie files: 2.4 MB, 2.3 MB, 3.3 MB, and 3.3 MB)

#73591 - $15.00 USD Received 2 August 2006; revised 15 September 2006; accepted 15 September 2006

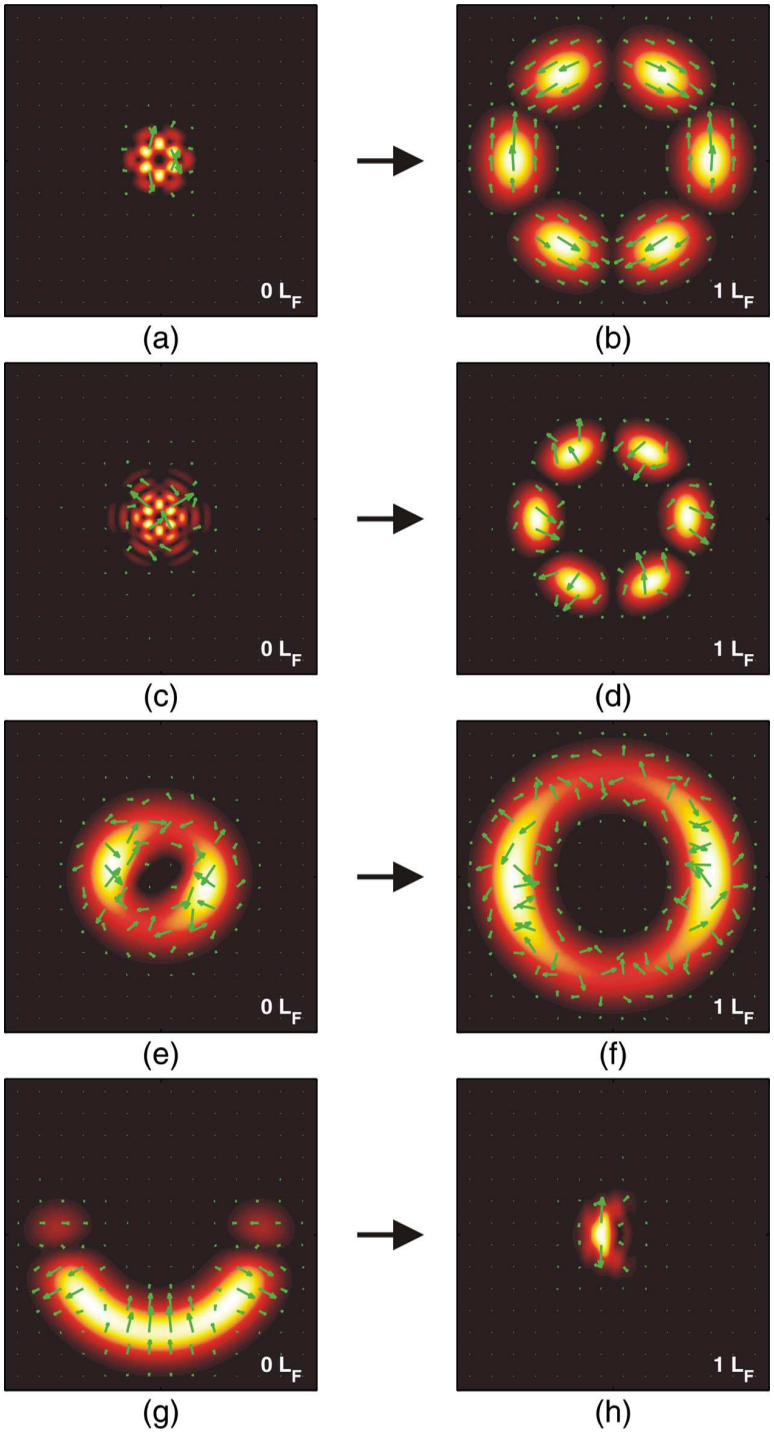

Fig. 3. Propagation of the transverse intensity distribution and electric vector field for generalized vector Bessel-cosine-Gauss, Mathieu-Gauss, and parabolic-Gauss beams. The parameter data for the propagations are included within the text. The movies show the evolution from $z = 0$ to $z = 4L_F$. (Movie files: 3.1 MB, 2.5 MB, 3.6 MB, and 2.2 MB)

#73591 - $15.00 USD Received 2 August 2006; revised 15 September 2006; accepted 15 September 2006

beams with even parity. The first propagation shown in Fig. 3(a) corresponds to a balanced input VBG beam of the form in Eq. (16) with seed function $W(\mathbf{r}_1) = iJ_3(\kappa_1 r_1)\cos(3\theta_1)$. The presence of the factor i in the seed function produces that, at the plane $z_2 = L_F$, the VBG beam be azimuthally polarized and belongs to the modified VHzG kind. The second propagation shown in Fig. 3(c) corresponds to a non-balanced VBG beam with $W(\mathbf{r}_1) = J_3(\kappa_1 r_1)\cos(3\theta_1)$ and complex input parameter $q_1 = 0.4 - i0.8/\sqrt{2}\pi$.

The propagation of a fourth-order helical vector Mathieu-Gauss (VMG) beam is shown in Figs. 3(e) and 3(f). The seed function is given by the superposition of even and odd Mathieu beams [11, 22], namely $W(\mathbf{r}_1) = \mathrm{Je}_4(\xi,3)\mathrm{ce}_4(\eta,3) + i\mathrm{Jo}_4(\xi,3)\mathrm{se}_4(\eta,3)$, where (ξ,η) are the elliptic coordinates defined as $x = f\cosh\xi\cos\eta$ and $y = f\sinh\xi\sin\eta$, with f being the semifocal distance. In this case the vector beam is balanced but the initial field belongs to the gVHzG kind with $\kappa_1 = 30 + i15\ \mathrm{mm}^{-1}$. The input field is given by Eq. (16) where the Cartesian partial derivatives are expressed in elliptic coordinates as follows

$$\frac{\partial}{\partial x} = \frac{1}{f\left(\cosh^2\xi - \cos^2\eta\right)}\left(\sinh\xi\cos\eta\frac{\partial}{\partial\xi} - \cosh\xi\sin\eta\frac{\partial}{\partial\eta}\right), \tag{25a}$$

$$\frac{\partial}{\partial y} = \frac{1}{f\left(\cosh^2\xi - \cos^2\eta\right)}\left(\cosh\xi\sin\eta\frac{\partial}{\partial\xi} + \sinh\xi\cos\eta\frac{\partial}{\partial\eta}\right) \tag{25b}$$

As the beam propagates, the parameters q and κ vary according to Eq. (23). For this value of κ_1, the typical elliptic annular intensity pattern of the ordinary helical VMG beams occurs approximately at $z \simeq 0.28L_F$, while the expected circular annular pattern of the modified helical VMG beams occurs at $z \simeq 1.28L_F$.

Finally, in Fig. 3(g) we show the propagation of a travelling vector Parabolic-Gauss (VPG) beam with TM polarization. The electric field is given directly by Eq. (7a) with a seed function given by the superposition of even and odd Parabolic nondiffracting beams [11, 23], namely $W(\mathbf{r}_1) = \mathrm{Pe}\left(u\sqrt{2\kappa}; p\right)\mathrm{Pe}\left(v\sqrt{2\kappa}; -p\right) + i\mathrm{Po}\left(u\sqrt{2\kappa}; p\right)\mathrm{Po}\left(v\sqrt{2\kappa}; -p\right)$ with parabolicity parameter $p = 2$. The Cartesian derivatives are expressed in the Parabolic coordinates $x = (v^2 - u^2)/2$, and $y = uv$ as follows

$$\frac{\partial}{\partial x} = \frac{1}{u^2 + v^2}\left(u\frac{\partial}{\partial u} - v\frac{\partial}{\partial v}\right), \tag{26a}$$

$$\frac{\partial}{\partial y} = \frac{1}{u^2 + v^2}\left(v\frac{\partial}{\partial u} + u\frac{\partial}{\partial v}\right), \tag{26b}$$

The beam is again balanced, but now we start the propagation assuming a purely imaginary $\kappa_1 = i30\ \mathrm{mm}^{-1}$ corresponding to a VPG of the modified kind. As expected for this initial condition, the beam now will belong to the ordinary kind at the plane $z_2 = L_F$.

To finish this section, let us remark that linearly polarized gVHzG beams can be also constructed as discussed in subsection 2.6. Since the propagation of these vector beams reduces to the propagation of scalar HzG beams, a variety of theoretical and experimental evolutions of linearly polarized gVHzG beams can be seen elsewhere, see for instance Refs. [11, 12, 26].

4. Conclusions

In this paper we have introduced a generalized form of the vector HzG beams that can be propagated in a closed and elegant form through axisymmetric paraxial optical systems characterized by ABCD transfer matrices. Once the choice of polarization of the transverse component is made, the propagation of the vector beams is completely characterized by the transformation of two independent complex parameters q and κ. The derivation of the new formulation

#73591 - $15.00 USD Received 2 August 2006; revised 15 September 2006; accepted 15 September 2006

has included the possibility of propagation in complex lenslike media having at most quadratic transverse variations of the index of refraction and the gain or loss.

Apart from a complex amplitude factor, the output field has the same mathematical structure as the input field, thus the gVHzG beams constitute a class of vector fields whose form is invariant under paraxial optical transformations. As a consequence, the transverse polarization of the gVHzG beams does not change under paraxial ABCD lossless transformations. This form-invariance property should not to be confused with the shape-invariance property of the scalar Hermite-Gauss or Laguerre-Gauss beams which preserve, excepting a scaling factor, the same transverse shape under paraxial lossless transformations. The intensity shape of the gVHzG beams will change because κ_1 and κ_2 are not proportional to each other through a real factor leading to different profiles of the function W, and moreover because the parameters q_1 and κ_1 are transformed according to different laws. Gaussian apodized fields with arbitrary polarization can be built up with a suitable superposition of constituent gVHzG beams with the same Gaussian envelope and transverse spatial frequency.

Acknowledgments

This research was supported by Consejo Nacional de Ciencia y Tecnología (grant 42808) and by Tecnológico de Monterrey (grant CAT007). M. A. Bandres acknowledge support from Secretaría de Educación Pública of México.

A. Appendix: Derivation of the output field $\mathbf{e}_2(\mathbf{r}_2)$ [Eq. (7a)]

By inserting $\mathbf{e}_1(\mathbf{r}_1)$ [Eq. (2)] into the Huygens diffraction integral Eq. (6) we obtain

$$\mathbf{e}_2(\mathbf{r}_2) = \frac{K\exp(iKL_0)}{i2\pi B}\iint_{-\infty}^{\infty} \mathrm{d}^2\mathbf{r}_1 \exp\left(\frac{iKr_1^2}{2q_1}\right)\exp\left[\frac{iK}{2B}\left(Ar_1^2 - 2\mathbf{r}_1\cdot\mathbf{r}_2 + Dr_2^2\right)\right] \times \nabla_1\left[\int_{-\pi}^{\pi}\mathrm{d}\phi\; g(\phi)\exp\left[i\kappa_1\left(x_1\cos\phi + y_1\sin\phi\right)\right]\right], \quad (27)$$

where $W(r_1;\kappa_1)$ has been already expressed using the expansion given by Eq. (3).

The gradient operator ∇_1 can be introduced within the angular integral and its application gives raise to two Cartesian field components, namely $\mathbf{e}_2(\mathbf{r}_2) = e_x\hat{\mathbf{x}} + e_y\hat{\mathbf{y}}$. Working with the x component we obtain the expression

$$e_x = \frac{K\exp(iKL_0)}{i2\pi B}\iint_{-\infty}^{\infty} \mathrm{d}^2\mathbf{r}_1 \exp\left(\frac{iKr_1^2}{2q_1}\right)\exp\left[\frac{iK}{2B}\left(Ar_1^2 - 2\mathbf{r}_1\cdot\mathbf{r}_2 + Dr_2^2\right)\right] \times i\kappa_1\int_{-\pi}^{\pi}\mathrm{d}\phi\; g(\phi)\cos\phi\exp[i\kappa_1(x_1\cos\phi + y_1\sin\phi)], \quad (28)$$

that can be rearranged as

$$e_x = \frac{K\kappa_1\exp(iKL_0)}{2\pi B}\exp\left(\frac{iKDr_2^2}{2B}\right)\int_{-\pi}^{\pi}\mathrm{d}\phi\; g(\phi)\cos\phi \times \iint_{-\infty}^{\infty}\mathrm{d}^2\mathbf{r}_1\exp\left[\frac{iKr_1^2}{2}\left(\frac{1}{q_1}+\frac{A}{B}\right)\right]\exp\left[-\frac{iK}{B}\mathbf{r}_1\cdot\mathbf{r}_2 + i\kappa_1(x_1\cos\phi + y_1\sin\phi)\right], \quad (29)$$

The double integral can be evaluated by splitting it into two single integrals and the result is

$$\frac{\pi}{a^2}\exp\left\{-\frac{1}{4a^2}\left[\left(\kappa_1\cos\phi - \frac{K}{B}x_2\right)^2 + \left(\kappa_1\sin\phi - \frac{K}{B}y_2\right)^2\right]\right\}, \quad (30)$$

#73591 - $15.00 USD Received 2 August 2006; revised 15 September 2006; accepted 15 September 2006

where $a^2 = -i\,(K/2)\left(q_1^{-1} + A/B\right)$.

Replacing Eq.(30) into Eq. (29) and after expanding the quadratic terms we obtain

$$e_x = \exp(iKL_0)\exp\left(-\frac{\kappa_1^2}{4a^2}\right)\exp\left(\frac{iKDr_2^2}{2B}\right)\exp\left(-\frac{K^2r_2^2}{4a^2B^2}\right) \times \int_{-\pi}^{\pi}\left[\frac{K\kappa_1}{2a^2B}\cos\phi\ \mathrm{d}\phi\right] g(\phi)\exp\left[\frac{K\kappa_1}{2a^2B}(x_2\cos\phi + y_2\sin\phi)\right]. \quad (31)$$

Now, from the expansion in Eq. (3), it is easy to identify that the integral corresponds indeed to the derivative of the function $W(\mathbf{r}_2;\kappa_2)$, then we have

$$e_x = \frac{\kappa_1}{\kappa_2}\exp\left(-i\frac{\kappa_1\kappa_2 B}{2K}\right) G(\mathbf{r}_2, q_2)\frac{\partial}{\partial x_2}W(\mathbf{r}_2;\kappa_2) \quad (32)$$

where the parameters q_2 and κ_2 are given by Eq. (9), $G(\mathbf{r}_2, q_2)$ is the fundamental Gaussian beam [Eq. (8)], and the unimodular condition $AD - BC = 1$ has been applied to eliminate D. The expression for e_y is also given by Eq. (32) with the difference that the partial derivative is now taken with respect to the y coordinate. Superposing both Cartesian components and using the gradient operator definition yields

$$\mathbf{e}_2(\mathbf{r}_2) = \frac{\kappa_1}{\kappa_2}\exp\left(-i\frac{\kappa_1\kappa_2 B}{2K}\right) G(\mathbf{r}_2, q_2)\nabla_2 W(r_2;k_2) \quad (33)$$

which is indeed Eq.(7a).

#73591 - $15.00 USD Received 2 August 2006; revised 15 September 2006; accepted 15 September 2006